

XIAN ESTÉVEZ-VENTOSA¹, NUBIA AURORA GONZÁLEZ-MOLANO²,
VANESA BLÁZQUEZ-PASCUAL², JOSÉ ALVARELLOS²,
LEANDRO R. ALEJANO^{1,3*}

A METHODOLOGY TO ESTIMATE PERMEABILITY IN POROUS AND FISSURED ROCK SPECIMENS AT LABORATORY SCALE

The correct management of underground works, petroleum and gas reservoirs and geothermal applications relies on the hydromechanical behaviour of rock masses. We describe a laboratory approach to measuring permeability for different types of rock specimens. A laboratory system was designed and set up using rock mechanics equipment (a servo-controlled hydraulic press, a Hoek cell, a pump for injecting water and a scale for measuring the volume of water flow). To verify the validity of the permeability measurements, tests were carried out on a reference porous rock (Corvio sandstone), with results showing good agreement with those published in the literature. Tests were subsequently carried out on artificially fissured granite specimens with different joint patterns, submitted to various confinement stresses up to 20 MPa. Results showed good agreement with traditional Klinkenberg test results. Other tests done with artificially fissured specimens are described for demonstrative purposes.

Keywords: Permeability, artificially jointed rock, lab tests

1. Introduction

A key feature of rock masses is their complex and discontinuous structure, directly related to their geological nature and tectonic history. An assessment of rock-mass hydromechanical behavior is crucial when managing complex projects such as underground works, petroleum and gas reservoirs, geothermal applications and stimulation developments.

¹ UNIVERSITY OF VIGO, DEPARTMENT OF NATURAL RESOURCES AND ENVIRONMENTAL ENGINEERING, SPAIN

² REPSOL TECHNOLOGY LABORATORY, MÓSTOLES, MADRID, SPAIN

³ VISITING SCHOLAR AT DEPARTMENT OF GEOLOGY AND GEOLOGICAL ENGINEERING, COLORADO SCHOOL OF MINES, GOLDEN, USA

* Corresponding author: alejano@uvigo.es



© 2020. The Author(s). This is an open-access article distributed under the terms of the Creative Commons Attribution-NonCommercial License (CC BY-NC 4.0, <https://creativecommons.org/licenses/by-nc/4.0/deed.en>) which permits the use, redistribution of the material in any medium or format, transforming and building upon the material, provided that the article is properly cited, the use is noncommercial, and no modifications or adaptations are made.

Bates & Jackson [1] defined permeability as ‘the property or capacity of a porous rock, sediment or soil for transmitting a fluid’; permeability, therefore, is a measure of the relative ease of fluid flow under unequal pressure. Fractured rock masses, including crystalline rocks, are variably permeable due to discontinuous structures mainly associated with discontinuities or joints. Because seepage flows in rock masses are governed by complex structural characteristics – such as discontinuity orientations, spacing, persistence, connectedness, joint infills, surface roughness and in-situ stress fields [2,3] – it can be difficult to estimate permeability. Engineers requiring crucial knowledge of permeability usually resort to in situ Lugeon, slug or pressure-pulse tests [4].

Several researchers have studied and proposed initial approaches to the laminar flow of a viscous incompressible fluid in a fracture [5-7]. Hoek and Bray [8] proposed a chart for estimating hydraulic conductivity in a rock mass based on inputting joint mean aperture and the average number of joints per metre and on computing hydraulic conductivity parallel to a set of clean, smooth parallel joints [9]. Hydraulic conductivity responds to the local cubic law (LCL), reflecting proportionality to the cube of joint aperture.

Witherspoon et al. [10] performed different tests in artificially induced rock fractures to check the validity of the LCL for open and almost closed joints subjected to different stress levels. However, the LCL is not always appropriate for describing hydraulic behaviour in natural fractures given that certain theoretical assumptions may not hold [11].

Alejano et al. [12] carried out rock mechanics stress-strain tests on artificially jointed rock specimens, treating them as small-scale artificial rock masses; on the same basis, it was considered useful to measure the permeability of specimens in the laboratory. Described, therefore, is a method for measuring permeability through saw-cut fractures in intact rock specimens and in intact porous rock specimens. The method uses adapted rock mechanics laboratory equipment consisting of a triaxial Hoek cell with pierced seat bases that allow water to flow through test specimens, a standard servo-controlled press framework, a hydraulic power supply and a scales that records the water outflow volume.

To verify the validity of the permeability measurements, tests were carried out on a reference rock (Corvino sandstone) and the results were compared with results reported in the literature [13]. Results for subsequent tests carried out on artificially fissured granite specimens presenting different joint patterns and undergoing different stress states were compared to Klinkenberg test results.

2. Laboratory equipment

Two test configurations were used so as to test specimens in different stress states. Note that it would also be possible to carry out tests with other different configurations by modifying the control parameters (confinement stress, axial stress and pore pressure). The configurations and methodology to calculate hydraulic conductivity are explained in what follows.

2.1. Test configuration

The tests to measure hydraulic permeability for porous intact and artificially fissured rocks required the following laboratory equipment:

- Standard triaxial cell, sizes NX and 1.5-inch (diameters 54 mm and 38.1 mm),
- A servo-controlled press framework as the source of axial stress (σ_1),

- A hydraulic power supply (designed by the authors),
- Spherical seat bases modified to allow water to be pumped through the specimen,
- Scales to automatically measure the pumped water volume,
- Linear variable differential transformer (LVDT) extensometers for strain measurement,
- Computer with suitable control and measurement software.

This equipment was used to build a system that injected water through the rock specimens and automatically measured mass, pressure and temperature (as desired) for the water used in the permeability tests for each stress state.

The measurement method was based on a standard triaxial test in which the axial pressure was set in two different ways: keeping constant the axial pressure value of $\sigma_2 = \sigma_3$, while increasing σ_1 from 1 MPa to 20 MPa; and setting the axial pressure value to the same value as the confinement pressure to induce an isotropic three-dimensional stress state in the test specimen ($\sigma_1 = \sigma_2 = \sigma_3$), while gradually increasing pressure from 1 MPa to 20 MPa and then reducing it back to 1 MPa. These approaches to testing minimized the possibility of damaging the specimens.

A standard Hoek cell was used in which the upper and lower spherical seat bases were modified so that pump-injected water above could be collected below after it passed through the porous or fissured specimen. The water entered a water distribution system under pressure through the upper seat base and, after passing through the specimen, was collected by a similar distribution system in the lower seat base, from where it exited to the scales through a plastic tube.

Since the water flowing out of the specimen through the lower base did so at atmospheric pressure, once the pressure value at the input point was fixed, the value of the differential pore pressure was known. Figure 1 depicts a diagram of the Hoek cell and dual-pump system, while Figure 2 shows photographs of the Hoek cell, spherical seat bases and water distribution elements.

Since water injection and control were critical to testing accuracy, we adapted a system to the needs of the tests that consisted of two pumps with connection circuits that allowed confinement

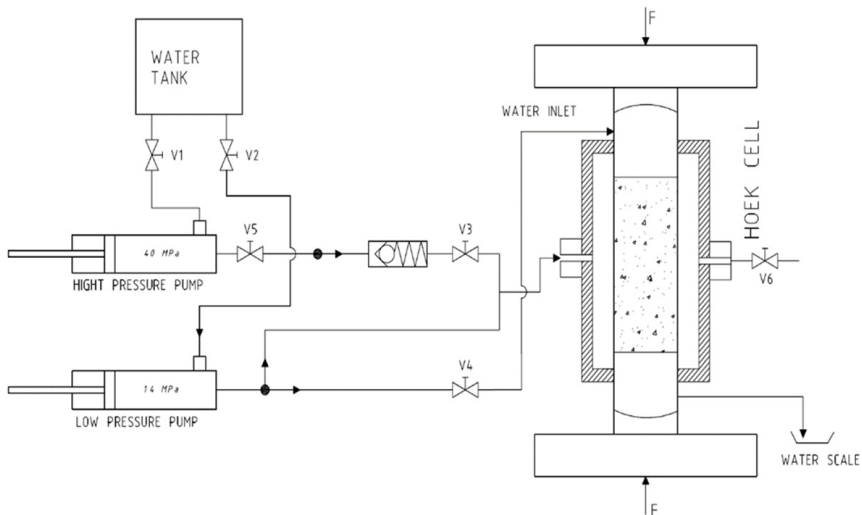


Fig. 1. Diagram showing the Hoek cell with hydraulic connections to the water input and outlet points and scales



Fig. 2. Photograph of the water injection system including the pumping system and the Hoek cell and spherical seat bases with water distribution elements

pressure to be exerted and water to be injected at the desired pressure. Once the low-pressure pump achieved working confinement pressure in the Hoek cell, the high-pressure pump took over, while the low-pressure pump switched to pumping water through the specimen at the desired pore pressure, as controlled and recorded by the system.

The triaxial stress state induced with the Hoek cell was typically of the type $\sigma_1 > \sigma_2 = \sigma_3$, where σ_1 corresponds to axial stress. Note that, with the Hoek cell, it was also possible to induce stress states such that the main stress was radial ($\sigma_1 = \sigma_2 > \sigma_3$). Regarding pore pressure u , the system was capable of injecting enough water to maintain pressure until the test was finished.

Finally, a specific software program was implemented to control and acquire data. The volume of water passing through the specimen per unit of time, pore pressure, confinement pressure, axial stress and (optionally) any deformations occurring during the test were recorded in an ad-hoc file. Note that the confinement stress, axial stress and pore pressure can also be servo-controlled, which means that different tests can be configured according to requirements.

2.2. Test methodology

The experimental test method consisted of measuring specimen dimensions, pore pressure and water volume flow in terms of time for different stress levels, i.e., as described above, keeping $\sigma_2 = \sigma_3$ constant while increasing σ_1 or maintaining an isotropic three-dimensional stress state ($\sigma_1 = \sigma_2 = \sigma_3$).

Data recorded during the test allowed the permeability of the tested specimen to be calculated, taking into account the assumption that linear Darcy's law holds, as in most cases of discontinuous water flow [14].

Applied was the unidirectional version of Darcy's law:

$$v[\text{m/s}] = k[\text{m/s}] \cdot i[-] \quad (1)$$

This law proportionally relates flow velocity v in m/s to hydraulic conductivity k in m/s and to the dimensionless hydraulic gradient i .

Water flow velocity through the specimen was calculated by taking into account the section of the specimen A [m²] and the water flowing through. Once the flow of pumped water was constant, the flow Q [m³/s] was estimated with data collected from the volume of water as measured by the scales and the time taken to pass through the specimen:

$$v[\text{m/s}] = \frac{Q[\text{m}^3/\text{s}]}{A[\text{m}^2]} \quad (2)$$

The hydraulic gradient was the waterhead Δh [m] divided by the height L [m] of the specimen:

$$i = \frac{\Delta h[\text{m}]}{L[\text{m}]} \quad (3)$$

The waterhead Δh related to water pressure u was computed as:

$$\Delta h[\text{m}] = \frac{u[\text{Pa}]}{\rho[\text{kg/m}^3] \cdot g[\text{m/s}^2]} \quad (4)$$

where ρ is water density at the test temperature and where g is gravity acceleration, taken as 9.81 m/s².

Once the velocity and hydraulic gradient values were known, permeability could be calculated using Eq. (1). Thus, intrinsic permeability could be computed as:

$$\kappa(\text{m}^2) = k \frac{\mu}{\rho g} = k[\text{m/s}] \frac{0.001[\text{kg/m} \cdot \text{s}]}{1000[\text{kg/m}^3] \cdot 10[\text{m/s}^2]} = k \cdot 10^{-7} [\text{m}^2] \quad (5)$$

where μ refers to water viscosity at ambient temperature. This intrinsic permeability value could also be expressed in darcies, taking $1 \text{ m}^2 = 1.013249966 \text{e} + 12$ darcies.

3. Laboratory tests

Once the test methodology was defined and all the equipment was assembled, preliminary tests were carried out aimed at fine-tuning the system. Several experiments were carried out on a reference rock whose permeability values were well known so that results for artificially jointed rock specimens could be compared to published results.

3.1. Reference rock specimen test

Using a reference rock for testing meant that the reliability of measurements made with the proposed method could be checked. Considering that the system was designed to calculate per-

meability in jointed rocks, the expected permeability values are of the order of 1 to 10^{-5} darcies. Selected as the reference rock was Corvicio sandstone which outcrops in the top section of the Frontada Formation in northern Spain (Lower Cretaceous) [15]. The permeability of this porous rock (with porosity in the range 15-20%) was estimated in three key directions for confinement levels by Canal Vila et al. [13], as shown in Figure 3, which also shows the values calculated by the described method.

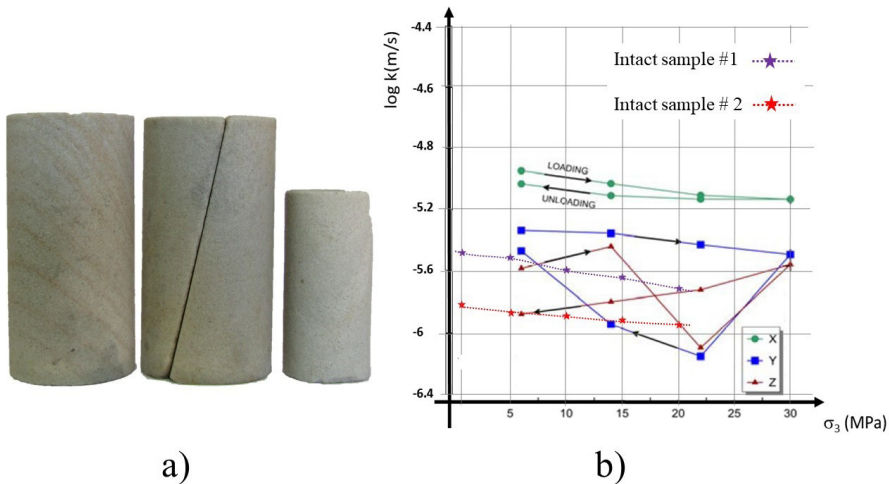


Fig. 3. a) Intact and fissured NX and 1.5-inch Corvicio sandstone test specimens. b) Hydraulic conductivity results for confinement increasing in three directions. Source: Adapted from Canal Vila et al. [13]

To carry out the control tests on the selected material, several NX (diameter 54 mm and double height) and 1.5-inch specimens were prepared and fully saturated by submergence in water for a week. The specimens were then tested by following the isotropic three-dimensional stress configuration of $\sigma_1 = \sigma_2 = \sigma_3$, gradually increasing pressure to 20 MPa in intervals of 1 MPa. Each pressure level was held constant until the flow of water injected through the specimen was constant, when flow could be measured in relation to time. Using this data and the described methodology, rock permeability was calculated for each level of confinement pressure. Figure 4a) shows the computed permeability results obtained for the three specimens, in the range 0.15-0.3 darcies; those values were as would be expected for very porous (15-20%) silica sandstone and were also in line with the results reported by Canal-Vila et al. [13]. An almost constant trend was observed, which would suggest that, due to the large pore size in the sandstone, the stress level did not significantly affect the permeability response [16].

To get an idea of the measurement capacity of the system, a specimen of the same reference material was prepared with a sub-vertical joint for testing (see Fig. 3) and, following the same procedure as described above, permeability was calculated for different confinement stress levels. Results are depicted in Figure 4a), which shows a relative increase in permeability in the fractured rock compared to the intact rock specimens. Note that an increase in stress leads the permeability value to fall in line with joint closure. Calculating the difference in permeability between fractured and unfractured rock gives mean permeability due to the rock joint. Finally,

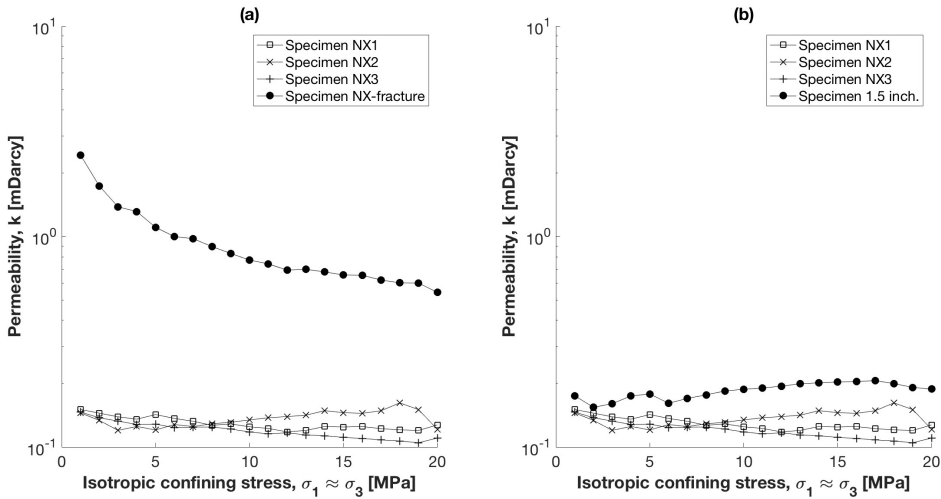


Fig. 4. Permeability evolution. a) Intact and artificially fissured sandstone specimens; b) Intact NX and 1.5-inch sandstone specimens

from the same reference material, a 1.5-inch double-height specimen was prepared and tested, with the goal of comparing the result obtained for this specimen with that obtained for the NX specimen. As can be seen in Figure 4b), the results compared quite well.

3.2. Fissured granite specimen test

For the purpose of testing the artificially fissured rock, four specimen types were prepared (Fig. 5), labelled 1+0 (one sub-vertical joint only), 1+2 (one sub-vertical joint and two sub-horizontal joints), 2+0 (two sub-vertical joints only) and 2+3 (two sub-vertical joints and three sub-horizontal joints). The specimen preparation procedure was as described in Alejano et al. [12].



Fig. 5. Photograph of the different types of artificially fissured (saw-cut) joints

To check the results obtained using the described method, preliminary manual tests were carried out on two type 1+2 specimens, with values for σ_1 and σ_3 held constant. The obtained results (see Table 1) were in the order of 0.01 darcys – a reasonable value for fissured granite [17,18]. The planned tests were therefore carried out and an automated test system was implemented.

TABLE 1

Stress conditions, water flow, hydraulic conductivity and permeability values from preliminary tests

Specimen	σ_1 [MPa]	σ_3 [MPa]	u [MPa]	Q [cm ³ /s]	k [m/s]	K [millidarcy]
NBM001	10	3	1.57	0.792	2.13e-7	21.6
NBM002	22	5	2.4	0.431	7.75e-8	7.9

3.2.1. Stress configuration 1 test

Two series of tests were performed for stress configuration 1, involving $\sigma_2 = \sigma_3$ being held constant while σ_1 was increased from 1 MPa to 20 MPa. This configuration meant that flow was forced in the direction of the main stress σ_1 and followed the sub-vertical joint. Type 1+2 specimens, with $\sigma_3 = 1$ MPa and $\sigma_3 = 2$ MPa, were used for the tests. Figure 6a) depicts the results, showing how permeability values remained more or less constant throughout the test and suggesting, therefore, that permeability was apparently not affected by the major principal stress.

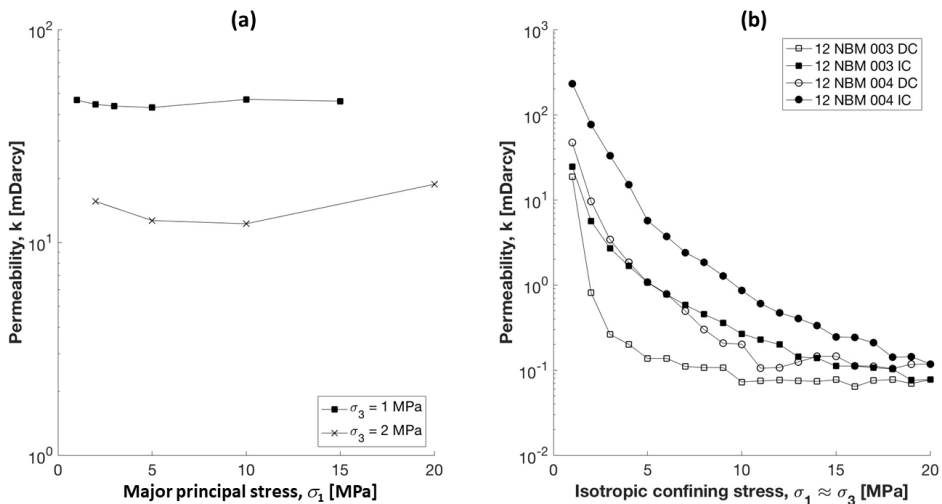


Fig. 6. Permeability test results. a) Stress configuration 1; b) Two type 1+2 specimens with loading from 1 MPa to 20 MPa and unloading from 20 MPa to 1 MPa (confinement increased in intervals of 1 MPa)

Considering that σ_1 did not seem to affect permeability, further tests were carried out for stress configuration 2, based on the isotropic three-dimensional stress state ($\sigma_1 = \sigma_2 = \sigma_3$).

3.2.2. Stress configuration 2 test

To carry out testing according to configuration stress 2, type 1+0, 1+2, 2+0 2+3 specimens were prepared. Automatic scheduling was performed on the system in that stresses were set to be equal ($\sigma_1 = \sigma_2 = \sigma_3$) and confinement was programmed to increase/decrease in regular intervals of 1 MPa. For a period of five minutes, confinement was held constant to obtain a constant flow of water through the specimen. During the test, lasting around three hours, the weight of the outflowing water was continually recorded by the system.

Using the obtained results and the approach described in Section 2, permeability evolution with confinement was estimated. Figure 6b) shows the permeability values obtained for loading and unloading for two type 1+2 specimens.

A clear trend of decreasing permeability and increasing confinement was evident, as reported elsewhere for in situ tests [10,17,18], with little difference between permeability values for loading and unloading, and very similar values by the end of the test. This hysteretic behaviour could be attributed to a suction effect in planar saw-cut joints. Differences could also be observed between the results obtained for the different specimens. Note that some difference is only to be expected even though the tests were carried out in the same way and with the same material; however, differences did not reach one order of magnitude and tended to mitigate with increased confinement. These differences may be associated with the interlocking or position of the blocks making up the complete fissured specimen.

Results for a full new series of five tests carried out on the type 1+0 specimens are shown in Figure 7a). The average permeability values are shown together with a potential function fitting those values. As with previous results, observed was the same trend of permeability values in the order of 10 millidarcies for lower confinements (1 MPa), and in the order of 0.05 millidarcies for higher confinements (20 MPa). In Figure 7b), which shows results obtained for the type 1+2 specimens, the same trend as for the type 1+0 specimens could be clearly observed. Note also

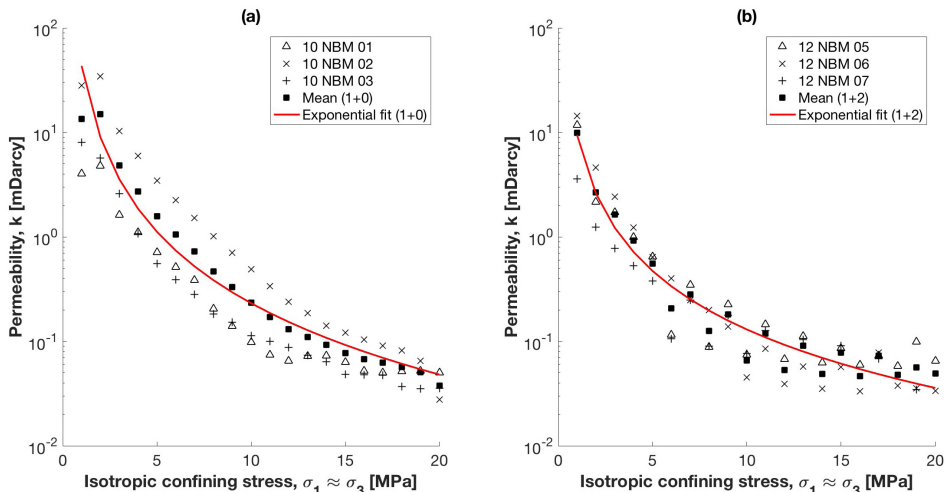


Fig. 7. Permeability test results for increasing confinement. a) Type 1+2 fissured specimens; b) Type 1+0 fissured specimens

that the permeability values obtained were of the same order of magnitude, tending to 0.05 millidarcys at higher confinements.

Similar tests were carried out on type 2+0 and 2+3 specimens, with results as depicted in Figure 8. The same evolution in permeability values could be observed, i.e., higher permeability values for lower confinements and vice versa. While permeability values of the same order of magnitude were obtained for the type 2+0 and 2+3 specimens, permeability was observed to be doubled for type 2+0 compared to type 2+3 specimens, particularly at lower confinement levels.

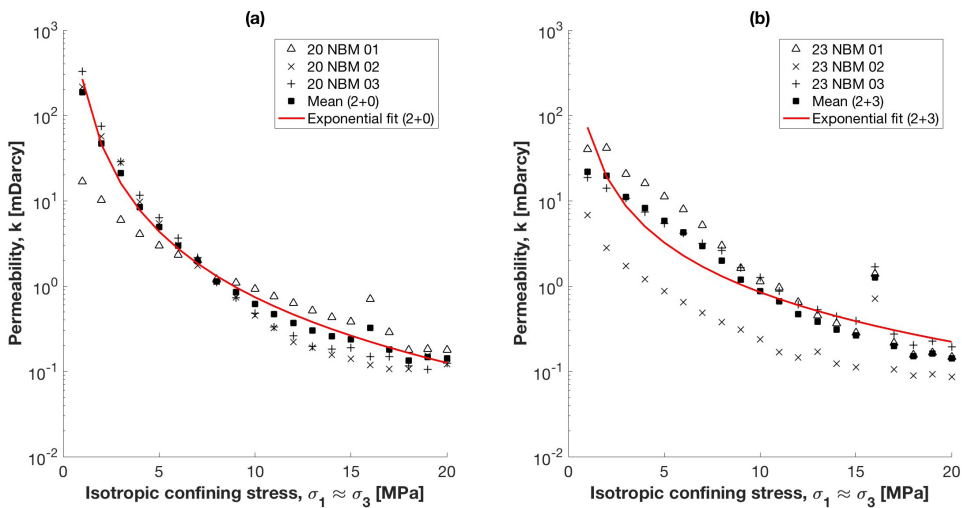


Fig. 8. Permeability test results for increasing confinement. a) Type 2+0 fissured specimens; b) Type 2+3 fissured specimens

To compare the obtained results, the exponential fits for each specimen type were graphed together. Figure 9a) shows that, while a similar response was obtained for all specimen types, two clear trends could be distinguished. The specimens with a single sub-vertical joint (types 1+0 and 1+2) were apparently less permeable than the specimens with two sub-vertical joints (types 2+0 and 2+3). Furthermore, for low confinement values, permeability was significantly higher in types 1+2 and 2+3 specimens than in types 1+0 and 2+0 specimens. This behaviour reflects the presence of sub-horizontal joints that make it difficult to assemble blocks in their correct position. Hypothetically, therefore, block movements occur that can close channels and obstruct flow in sub-vertical joints, which does not happen in the case of specimens without sub-horizontal joints. This effect seemed to be mitigated when confinement pressure was increased. At higher confinement values (20 MPa), permeability tended to be similar for each group of specimens – at roughly 0.05 millidarcys for types 1+0 and 1+2 – but is around three times higher (about 0.14 millidarcys) for types 2+0 and 2+3. The fact that specimens with two sub-vertical joints are more permeable than those with only one sub-vertical joint makes sense, although it should be noted that the difference lies within the range of variability detected in the measurements for each specimen group.

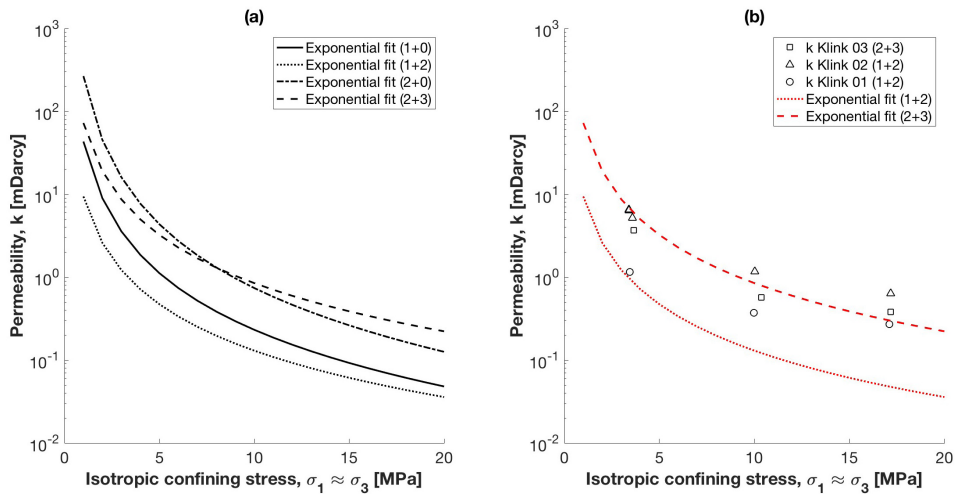


Fig. 9. a) Comparison of permeability test results for types 2+0, 2+3, 1+0 and 1+2 specimens;
 b) Comparison of permeability test results for water and gas (Klinkenberg correction)

4. Comparative Klinkenberg permeability testing

To verify the proposed method, standard measurement equipment was used to compute permeability for prepared type 1+2 and 2+3 specimens. Gas permeability was measured using the AP-608 automated permeameter-porosimeter (Coretest Systems), following the unsteady-state method with pressure fall-off [19]. This set-up has a 1.5-inch isotropic core holder that uses water to apply confining pressure and N₂ as the fluid passing through the specimen.

The gas permeability results obtained after the Klinkenberg [20] correction are shown in Figure 9b), together with the fit previously obtained for specimen types 1+2 and 2+3. As can be seen, gas permeability values were quite similar to those computed following the method described in Section 2. Note that for high pressure values, permeability for gas was slightly higher than that obtained for water, but still remained within the found range of variability.

5. Measuring permeability in specimens with non-planar fissures

The described permeability approach was tentatively applied to specimens with artificial joints differently induced by means of shear or tensile stress instead of by saw-cutting. Figure 10 depicts the results and images of the tested specimens.

The same trend was evident as described above, although the permeability values obtained were higher. This was because the increased roughness in the joints produced more flow channels than was the case for the saw-cut specimens. We suggest that more tests and a better characterization of surface roughness are needed to be able to draw definitive conclusions. These initial results, however, sustain the feasibility of this type of testing, which was the result sought at this stage of the authors' research.

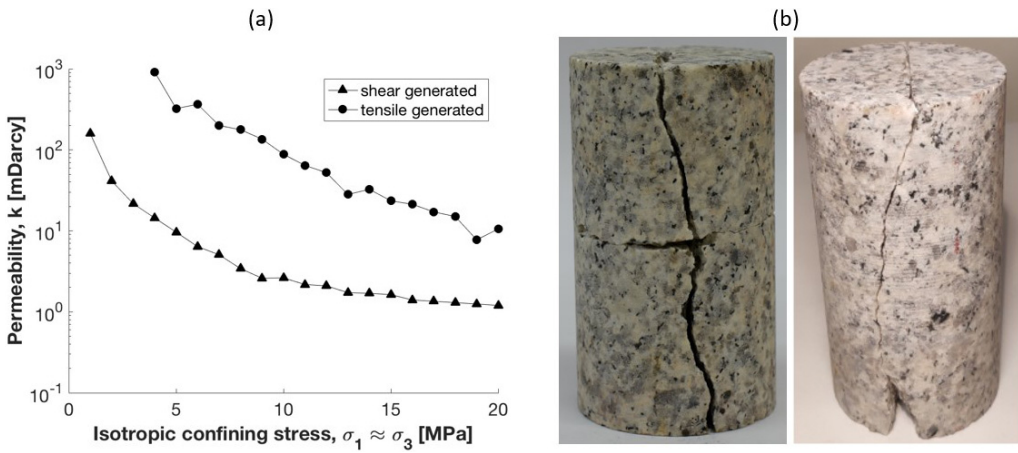


Fig. 10. Permeability results (a) for different isotropic stress levels for tensile-stress and shear-stress artificially jointed specimens (b)

6. Conclusions

A relatively elementary system and methodology has been described to compute permeability in rock specimens at different stress levels. Standard rock mechanics laboratory equipment was adapted by including a water injection system to force water to flow through the test specimen and a scales to measure water flow. This system allows water flow through porous rocks and fissured rocks to be measured under different stress conditions. Also implemented was a control system to configure the different variables (confinement pressure, injection pressure, etc).

To test the validity of the method and its results, a homogeneous porous reference rock (Corvio sandstone) was tested in two specimen sizes (NX and 1.5 inches). Also tested in this sandstone was a specimen with a sub-vertical artificial joint. The test results compared well with known permeability data.

A number of tests were carried out in artificially jointed granite specimens with differing numbers of saw-cut joints. Evident was dependency between the permeability value and the number of joints that favoured the flow of water. Results for the developed method compared to standard Klinkenberg permeability test results showed good agreement. Reasonable permeability values were also obtained for shear-stress and tensile-stress artificially jointed specimens.

This relatively simple system, which has been shown to be capable of measuring permeability in specimens of porous rock, specimens of rock with different types of joints and specimens of rock with different stress configurations, will be further tested in other research scenarios.

Acknowledgements

This experimental work was funded by REPSOL S.A. The first and last authors acknowledge the Spanish Ministry of Universities for funding of the project, awarded under Contract Reference No. RTI2018-093563-B-I00, partially financed by means of ERDF funds from the EU.

References

- [1] R.L. Bates, J.A. Jackson, *Glossary of Geology*, 3rd ed. American Geol. Inst., Alexandria, Virginia, USA (1987).
- [2] C.H. Lee, I. Farmer, *Fluid flow in discontinuous rocks*, Chapman & Hall, London (1993).
- [3] M. Wierzbicki, P. Konečný, A. Kožušnicková, *Arch. Min. Sci.* **59** (4), 1131-1140 (2014).
- [4] National Research Council, *Rock fractures and fluid flow: contemporary understanding and applications*. National Academy Press, Washington DC (1996).
- [5] J. Boussinesq, *J. Math. Pure. App. Ser. 2* (13), 377-424 (1868)
- [6] C. Louis, *Imp. Coll. Sci. Techno.* 90 pp (1969).
- [7] J. Bear, *Dynamics of Fluids in Porous Media*, Elsevier, New York (1972).
- [8] E. Hoek, J. Bray J, *Rock slope engineering* (2nd ed.). The Institution of Mining & Metallurgy, London, UK (1974).
- [9] S.N. Davis, Porosity and permeability of natural materials. In: *Flow through Porous Media* (ed. R. de Weist) Academic Press, London, pp. 54-89 (1969).
- [10] P.A. Witherspoon, J.S.Y. Wang, K. Iwai, J.E. Gale, *Water Resour. Res.* **16**: 1016- 1024 (1980)
- [11] V. Tzelepis, K.N. Moutsopoulos, J.N.E. Papaspyros, V.A. Tsihrintzis, *J. of Hydrol.* **521**, 108-118 (2015).
- [12] L.R. Alejano, J. Arzúa, N. Bozorgzadeh, J.P. Harrison JP, *Int. J. Rock. Mech. Min. Sci.* **95**, 87-103 (2017).
- [13] J. Canal-Vila, I. Falcón-Suárez, V. Barrientos, J. Delgado-Martín, *Macla (Rev. Soc. Esp. Miner.)* ISSN 1885-7264, **17**, 31-32 (2013).
- [14] W. Wittke, *Rock mechanics based on an anisotropic jointed rock model (AJRM)*. John Wiley & Sons. New Jersey (2014).
- [15] J.M. Hernández, V. Pujalte, S. Robles, C. Martín-Closas C, *Rev. Soc. Geol. Esp.* **12**, 377-396 (1999).
- [16] Y. Bernabé, *Geoph.* **56**, 436-446 (1991).
- [17] G. Gustafson, *Hydrogeology for rock engineers*. BeFo. Stockholm (2012).
- [18] J. Rutqvist, O. Stephansson, *Hydrogeol. J.* **11** (1), 7-40 (2003).
- [19] S.C. Jones. *Soc. Pet. Eng. J.* **12** (5), 383-397 (1972).
- [20] L.J. Klinkenberg, *The permeability of porous media to liquids and gases*. API Drilling and Production Practice, 200-213 (1941).